

Electric field control and analyte transport in Si/SiO₂ fluidic nanochannels

Yi Zhang,^{†a} Thomas C. Gamble,^{†a} Alexander Neumann,^b Gabriel P. Lopez,^a Steven R. J. Brueck^{b,c} and Dimiter N. Petsev^{*a}

Received 12th March 2008, Accepted 16th July 2008

First published as an Advance Article on the web 29th August 2008

DOI: 10.1039/b804256j

This article presents an analysis of the electric field distribution and current transport in fluidic nanochannels fabricated by etching of a silicon chip. The channels were overcoated by a SiO₂ layer. The analysis accounts for the current leaks across the SiO₂ layer into the channel walls. Suitable voltage biasing of the Si substrate allows eliminating of the leaks or using them to modify the potential distribution of the fluid. Shaping the potential in the fluid can be utilized for solute focusing and separations in fluidic nanochannels.

Introduction

The transport of fluid, current and solutes in fluidic nanochannels presents a significant fundamental and practical interest.^{1–9} As the dimensions of the channels reach the range between a few nanometres and a few hundreds of nanometres, they become comparable to the size of the electric double layer that usually forms at channel walls.^{10,11} The double layer thickness is a measure of the typical range of the electrostatic potential that propagates from the wall into the liquid and depends on the electrolyte concentration and valence.¹² Thus for an aqueous solution of symmetric 1 : 1 electrolyte, such as KCl, with concentrations varying between 0.01 and 10^{–6} M, the double layer thickness would change from 3 to 300 nm. For asymmetric 2 : 1 electrolyte, such as MgCl₂, and the same concentrations the respective double layer thicknesses vary between 1.8 and 18 nm while for symmetric 2 : 2, such as MgSO₄, the corresponding range is 1.5 to 15 nm. Channels that are less than a few nanometres in size require a description of the molecular structure of the fluid.^{13–22}

The ionic and molecular transport in channels that are comparable to the double layer thickness is strongly affected by the electrostatic potential.^{10,11,23} For example, electroosmotic fluid flow distribution $v_{eo}(x)$ in such channels follows the shape of the potential in the electric double layer $\Psi(x)$, *i.e.*

$$v_{eo}(x) = -\frac{\varepsilon\varepsilon_0\zeta E}{\eta} \left[1 - \frac{\Psi(x)}{\zeta} \right] \quad (1)$$

ε_0 is the dielectric constant of free space, ε is the relative dielectric permittivity of the solution, η is its viscosity, ζ is the electrokinetic zeta potential and x is the transversal coordinate

across the channel.⁹ The quantity E denotes the externally applied electric field. At the same time all dissolved ionic species are distributed according to their charge: counterions accumulate in the immediate vicinity of the charged channel wall while the co-ions are repelled toward the center according to the Boltzmann distribution⁹

$$c(x) = c_0 \exp \left[-\frac{z_A e \Psi(x)}{kT} \right] \quad (2)$$

$c(x)$ is the local concentration, c_0 is the concentration in the reservoirs in fluidic contact with the channel, z_A is the charge number of the analyte and e is the electron charge. The electrophoretic transport of the analyte is given by $v_{ep}c(x)$ where ζ_A is the electrokinetic zeta potential of the analyte^{10,11}

$$v_{ep} = \frac{\varepsilon\varepsilon_0\zeta_A}{\eta} \quad (3)$$

The strong double layer effects present in small channels imply that manipulating the electrokinetic ζ -potential at the channel wall is a convenient tool for transport control. The ζ -potential modulation can be achieved by applying a voltage bias at the wall by means of an additional electrode. In this way the device operates as a fluidic field effect transistor. This idea was originally suggested by Ghowsi and Gale^{24–26} and applied for electroosmosis in micron-sized channels. It has only been recently used to execute transport control and manipulation in fluidic nanochannels.^{2–4} Alternatively, if one can manipulate the electric field E along the channel it will also be possible to manipulate the transport of the charged analytes (see eqn (1) and (3)).

Nanochannels are often fabricated on silicon wafers utilizing techniques developed in the microelectronic industry such as high resolution lithography and anisotropic etching.^{7,9,27–31} The channels are then covered with SiO₂ to insulate the solution from the silicon substrate. However, SiO₂ is not a perfect insulator^{32,33} and current may leak across into the underlying substrate (see Fig. 1a). As the channel width approaches the nanometre range, its resistance increases and may become comparable or even exceed that of the oxide layer. Hence, for a wide range of

^aCenter for Biomedical Engineering and Department of Chemical and Nuclear Engineering, University of New Mexico, Albuquerque, NM, 87131, USA. E-mail: Dimiter@unm.edu; Tel: +1-(505) 277-3221

^bCenter for High Technology Materials, University of New Mexico, Albuquerque, NM, 87106, USA

^cDepartment of Electrical and Computer Engineering, University of New Mexico, Albuquerque, NM, 87131, USA

[†]These authors equally contributed to the paper.

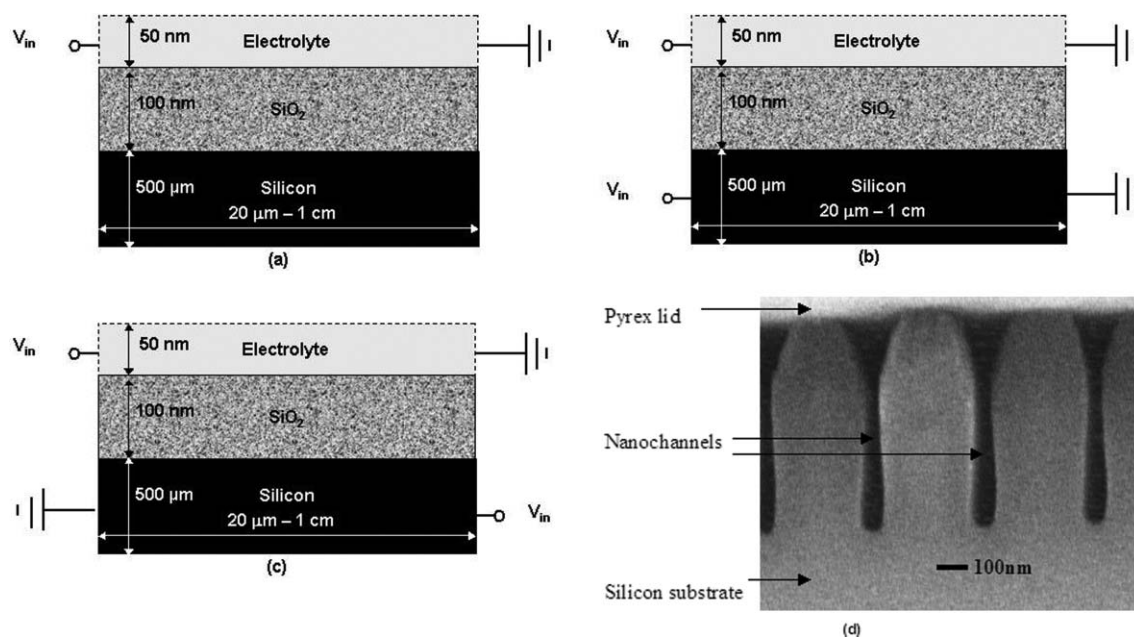


Fig. 1 A sketch of a fluidic nanochannel in Si/SiO₂ substrate. Only half of the channel is depicted since the boundary is a line of symmetry corresponding to the center of the channel. (a) Nonbiased Si substrate. (b) The Si substrate is biased by applying a collinear field to that in the electrolyte. (c) The Si substrate is biased with an oppositely directed field. The dimensions are typical but may be controllably varied depending on the fabrication protocol. (d) SEM micrograph of nanochannel cross-section. The nanochannels were approximately 450 nm tall and having an average width of approximately 70 nm. This end of the channel array is in fluidic contact with the solution reservoir.

channel dimensions and oxide layer thicknesses, the current will be predominantly transported across the SiO₂ layer into the Si substrate. This fact leads to a nonlinear potential distribution, or equivalently, a variable electric field along the fluidic channel. The transport phenomena that occur in such a system will be very different than those in a regular electrokinetic cell where such current leaks are not present or are insignificant and the field driving the transport is constant.

In this paper, we present numerical analysis of the transport of current in a 2-dimensional fluidic slit fabricated in a Si/SiO₂ substrate. We identify the parameters that govern the current leaks across the SiO₂ layer and quantify their impact. It is also demonstrated that the SiO₂ conductivity can be exploited to controllably shape the electric field inside the fluidic nanochannel thus providing an additional methodology for transport control. Hence, our study is focused on manipulating the applied electric field E through the current that leaks across the SiO₂ into the Si substrate. This is a different approach from the one that manipulates the channel wall potential.^{2-4,24-26} We have also performed experiments to validate the theoretical model.

Theory

The system that we model is shown in Fig. 1. The electrolyte solution, SiO₂ and Si are conductive. The SiO₂ layer is also characterized by capacitance. The contribution of the electroosmotic current is assumed to be negligible in comparison with that due to ionic migration and leakage across the oxide layer. This assumption is reasonable for channels that are much smaller than the electric double layer where the ionic migration is more significant.³⁴ Then the whole system can be analyzed in the framework of the Maxwell electrodynamics equations, which account for both conductivity and transient capacitance effects³⁵

$$\begin{aligned} \nabla \cdot (\epsilon \epsilon_0 \mathbf{E}) &= \rho_c, \mathbf{E} = -\nabla V \\ \frac{\partial \rho_c}{\partial t} &= -\nabla \cdot \mathbf{J}, \mathbf{J} = \sigma \mathbf{E} \end{aligned} \quad (4)$$

E is the electric field, V is the electric potential distribution due to the externally applied voltage, ϵ and ϵ_0 are the relative dielectric constant and the permittivity of free space respectively, ρ_c is the local charge density, \mathbf{J} is the current, and σ is the conductivity that corresponds to each region. Then eqn (4) can be reduced to

$$\begin{aligned} \nabla \cdot \frac{\partial}{\partial t} (\epsilon \epsilon_0 \nabla V) + \nabla \cdot (\sigma \nabla V) &= 0 \\ \nabla \cdot (\sigma \nabla V) &= 0 \quad (\text{for stationary current}) \end{aligned} \quad (5)$$

Eqn (5) is numerically solved using the COMSOL 3.3 package (COMSOL, Inc.) An important consideration is that the conductivity for SiO₂ is not a constant, but depends on the local voltage.^{32,33} We measured the conductivity of Si/SiO₂ in contact with electrolyte solution as a function of the direct current voltage applied to the silicon substrate as shown in Fig. 2. The shape of the curve supports the notion that the conductivity is a function of the applied voltage.^{32,33} These data are interpolated and the result then introduced as the voltage dependent conductivity $\sigma(V)$ in eqn (5). The latter is numerically solved for all the domains depicted in Fig. 1 with the respective boundary conditions shown therein. The boundary conditions at the electrolyte/SiO₂ and SiO₂/Si interfaces correspond to current conservation. All the rest of the boundaries are considered to be insulated except for the those that have the electrodes that supply the external field. These boundaries are set at the voltage and ground as shown in Fig. 1. The model does not account for the fluid motion due to electroosmosis¹¹ as well as for the

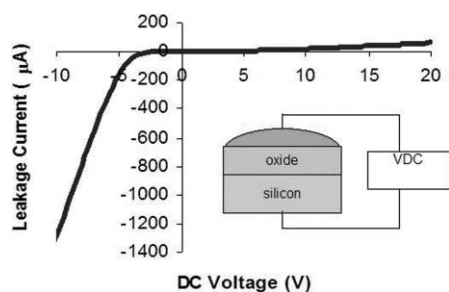


Fig. 2 Experimental current vs. voltage curve for electrolyte/SiO₂/Si system. The SiO₂ layer thickness is 100 nm. The voltages on the horizontal axis refer to the electrode that is connected to the Si substrate. The electrode in the fluid is ground.

electromigration and diffusion of charged species. An essential feature of this system is that the external field E may not be constant along the channels due to the current leaks across the SiO₂ layer. Therefore, field gradients might form which allows the focus of analytes at specific locations.

We first analyze the current flow distribution as a function of the channel length. This is important because it defines the experimental limitations of these systems. Fig. 3 shows the relative current transported along the electrolyte solution layer

and across the SiO₂ into the silicon. The electrodes are connected only to the fluidic channel as shown in Fig. 1a. Short channels do not exhibit any effects of current leaks across the SiO₂ layer (see Fig. 3a). Increasing the channel length leads to greater resistance of the fluid while the conductivity of the oxide layer does not change. This is because the current across the oxide layer depends on its thickness and morphology, which clearly does not change with the channel length. For very long channels most of the current leaks across the SiO₂ (see Fig. 3b). Hence for a 100 nm thick SiO₂ layer with the conductivity depicted in Fig. 2, all of the current is transported through the fluid if the channels are 20 µm or shorter (see Fig. 3a). Compared to the fluidic channel width (100 nm), the length is still very significant and the aspect ratio (length/width) is very large. On the other hand, if the channel length is about 1 cm or more, there is no current carried along by the fluid except very close to the channel inlet and outlet where the current flows from or to the electrodes into the liquid (see Fig. 3b). The dependence of the current leak on the total channel length is shown in more detail in Fig. 3c. The current transported by the fluid in the presence of leaks across the SiO₂ is normalized by the current in a perfectly insulated channel. The ratio is then plotted against the channel length. Fig. 3c suggests that the current leaks become dominant for channel lengths ~1 mm.

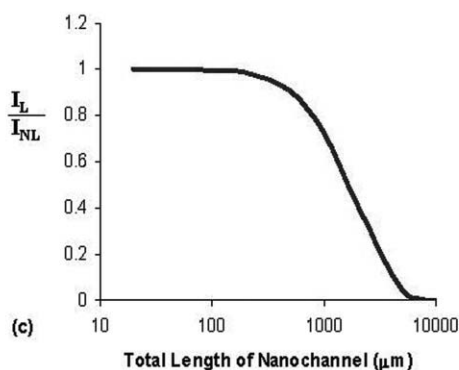
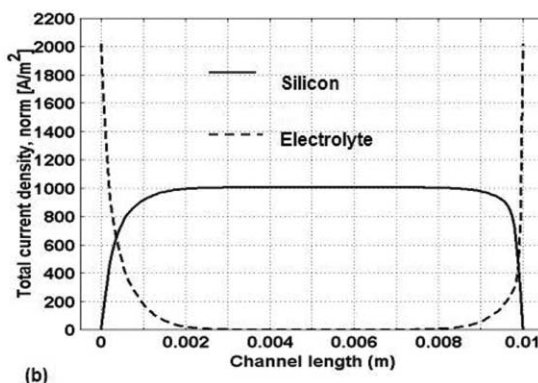
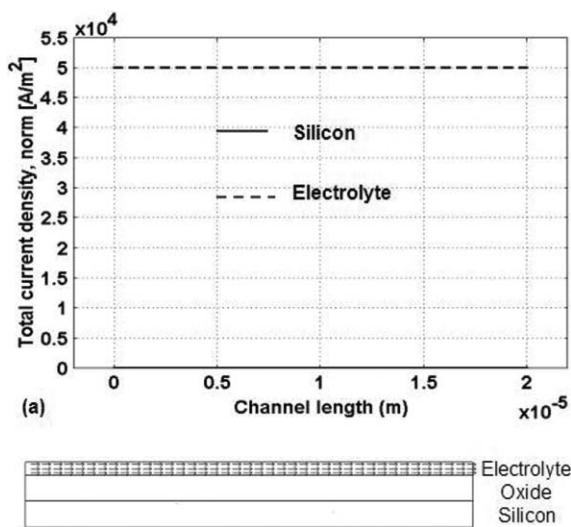


Fig. 3 Current density in nanofluidic channels in Si/SiO₂ substrate. The applied potential difference is 20 V. The lines correspond to the current density in the midplanes of the fluidic channel and the Si substrate. The fluidic channel width is 100 nm, the SiO₂ thickness is also 100 nm and the Si substrate is 500 µm thick. (a) The channel length is 20 µm; (b) the channel length is 1 cm; (c) plot of the ratio of the current in a leaky nanochannel I_L over the current in a non-leaky nanochannel I_{NL} versus the total length of the nanochannel.

This critical length will vary with the relative conductivities of the fluid and the SiO₂ layer. The critical channel lengths will increase with the solution conductivity and will decrease with the oxide layer conductivity. Hence, for channels longer than 1 mm the electric field within most of the channel interior will be essentially zero (the rest of the dimensions are given in Fig. 1). For longer channels the electric field within most of the channel interior will be essentially zero. However, there will be very large fields at the channel entrance and the exit. Therefore, there will be no electrophoretic and electroosmotic effects in the channel center. At the same time, the electroosmotic driving forces at the channel ends, where the fields are substantial can result in fluid pumping. This is because the overall electroosmotic flow along a channel does not depend on the local potential distribution (or electric field) but only on the potential difference between the electrodes at the two ends.³⁶ The fluid flow profile far from the electrodes will have the typical pressure driven parabolic shape. This fact can be exploited for separation of species based on their charge. Charged molecules with the same polarity as the wall will be repelled toward the center where they will move faster, while uncharged ones will be uniformly distributed across the channel and on the average will lag behind.⁹ We have ignored the contribution of the electroosmotic convection in comparison with the ionic electromigration and leaks through the SiO₂ layer since it is much smaller for very narrow channels.³⁴ This means that it does not have a substantial effect on the field *E* in the channel. However, we have to take into account the convection of dissolved analytes. This is because it may be the only mode of analyte transport, particularly in the regions where the field *E* is low. Hence, the convective current does not have a strong effect on the field distribution, since the latter is dominated by current transport and leaks into the oxide. The convective fluxes are dominant in cases where the field is very low (because of current leaks—see Fig. 3b).

The current leak across the SiO₂ layer can be entirely eliminated if the silicon substrate is subjected to the same voltage drop as the electrolyte solution along the fluidic channel (see Fig. 1b). In this case there is no voltage drop across the SiO₂ layer and hence no driving force for current. Then the potential drop in the liquid will be unperturbed and strictly linear, which corresponds to a constant and uniform electric field (see Fig. 4a). This situation will be analogous to that found in capillary electrophoresis separations that are conducted at a larger scale. In nanochannels, however, the strong electric double layer overlap may lead to different possibilities for molecular manipulation and separation.⁹

A very interesting case is when the liquid channel and the Si substrate layer are subjected to voltage drops with opposite polarity. Such a voltage arrangement leads to a complex shape of the voltage distribution along the channel. This gives rise to a range of opportunities for charged analyte manipulation like focusing or displacement from certain regions of the channel. In general, nonlinear electric fields can present very suitable conditions for solute separations or focusing.^{36–38} An example for such a non-uniform field is depicted in Fig. 4b where the fluidic channel and the underlying Si substrate are subjected to voltages as shown in Fig. 1c. In this case the voltage distribution in the solution is a function of that in the Si substrate across the SiO₂ layer. More complex potential distributions in the substrate

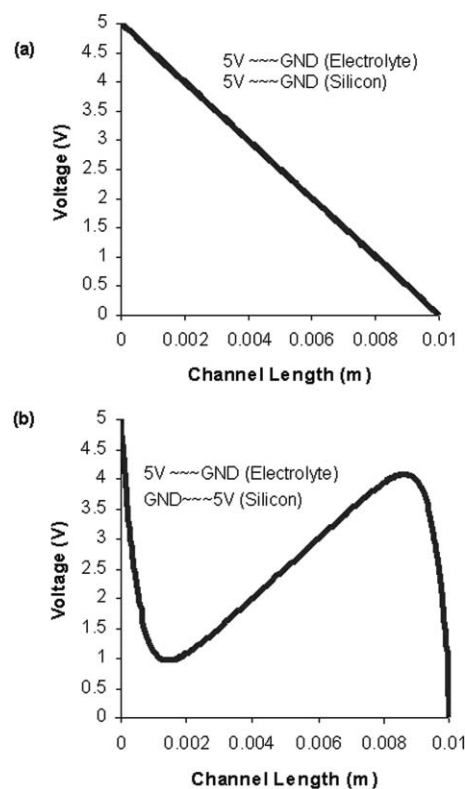


Fig. 4 Potential distribution in a fluidic channel. (a) Parallel Si substrate biasing (see Fig. 1b). (b) Antiparallel Si substrate biasing (see Fig. 1c) GND = ground.

(e.g., obtained by using multiple electrodes in contact with the Si substrate) would allow for even more complicated shapes of the potential distribution in the solution layer.

Experiment: focusing of a charged analyte

We have tested our theoretical model by performing an experiment in a model nanochannel system. The measurements were conducted in an array of 1000 identical channels that run in parallel. This makes the observation of the dye in the nanochannels easier and more reliable.⁹ The nanochannel was initially filled with 0.5 mg ml⁻¹ Alexa 488 dye (Invitrogen) in Tris-Glycine buffer at pH 8.3. Alexa 488 has a -2 charge at this pH. The voltages in the liquid are +5 V (left) and ground (right). The Si substrate has the opposite voltage setting: ground (left) and +5 V (right)—see Fig. 1c. At these settings the potential in the fluidic channel would acquire a shape similar to the one in Fig. 4b. The experimental results are presented in Fig. 5. The charged molecules experience convective electroosmotic transport from left to right as shown in the picture. Due to conservation, the electroosmotic flow does not depend on the local potential distribution but only on the voltages on both ends of the channel (see ref. 9). The electrophoretic migration of the charged species, on the other hand, is sensitive to the local field. The negatively charged molecules will be subjected to electrophoresis that depends on the local field strength (potential slope). In the region with positive potential slope (in the middle of the channel) the negative species will electrophoretically migrate in the same direction as the electroosmotic flow. The potential slope at the two ends of the channel, however, is

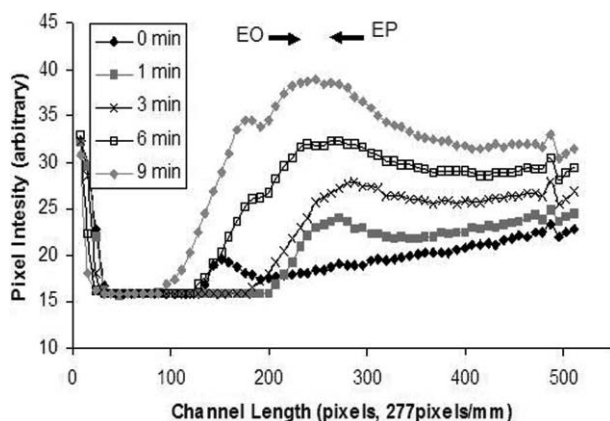


Fig. 5 Increase of the concentration of charged dye Alexa 488 due to a balance between the electroosmotic (EO) convective flux and the electrophoretic (EP) migration.

negative and the molecules will migrate in the direction that is opposite to the electroosmotic flow (*i.e.* right to left). There, the two fluxes will balance leading to molecular focusing. Such focusing is shown in Fig. 5. It represents the region in the vicinity of the left reservoir in fluidic contact with the nanochannel. The total length that is presented is ~ 1.8 mm. Note that the electroosmotic flow is not necessary for the focusing of the charged molecules. In absence of fluid motion (*e.g.* when the channel walls have no charge) the molecules will focus exactly at the extremum of the potential driven by electrophoresis. The effect of electroosmosis is a slight displacement of the concentration maximum from the electric potential extremum.

Conclusions

Electrokinetic effects dominate the transport in fluidic nanochannels.²³ Hence, the overall magnitude and shape details of the electrostatic potential distribution are extremely important for the performance of a nanofluidic device. We have demonstrated that nanochannels fabricated in Si and then covered with SiO₂ are prone to current leaks from the fluid into the Si substrate. The relative magnitude of the leaks depends on the channels dimensions (length and cross-section), the SiO₂ properties (thickness and morphology) and the magnitude of the applied voltages. The current leaks could be undesired in many cases because they deform the electric field along the fluidic channel. An approach to completely eliminate this field distortion by an appropriate (parallel) voltage bias applied to the underlying Si substrate is suggested. We also demonstrate that the current leakage effect and the SiO₂ capacitance can be used to shape the potential distribution and electric field along the channels in specific ways and then utilized for solute manipulation such as preconcentration, focusing and separations.

Acknowledgements

The authors appreciate the helpful discussions with Drs Cornelius F. Ivory (Washington State University) and Sang Han (University of New Mexico). This work has been supported by the NSF (NIRT: CTS 0404124, and PREM: DMR 0611616), the

Center for Biomedical Engineering at UNM and the W. M. Keck Foundation.

References

- 1 M. B. Stern, M. W. Geis and J. E. Curtin, *J. Vac. Sci. Technol., B*, 1997, **15**, 2887.
- 2 R. Fan, M. Yue, R. Karnik, A. Majumdar and P. Yang, *Phys. Rev. Lett.*, 2005, **95**, 086607.
- 3 R. Karnik, R. Fan, M. Yue, D. Li, P. Yang and A. Majumdar, *Nano Lett.*, 2005, **5**, 943.
- 4 R. Karnik, K. Castelino and A. Majumdar, *Appl. Phys. Lett.*, 2006, **88**, 123114.
- 5 S. Vankrunkelsven, D. Clicq, D. Cabooter and W. De Malsche, *J. Chromatogr., A*, 2006, **1102**, 96.
- 6 R. B. Schoch, A. Bertsch and P. Renaud, *Nano Lett.*, 2006, **6**, 543.
- 7 J. Han, S. W. Turner and H. G. Craighead, *Phys. Rev. Lett.*, 1999, **83**, 1688.
- 8 M. A. Burns, B. N. Johnson, S. N. Brahmasandra, K. Handique, J. R. Webster, M. Krishnan, T. S. Sammarco, P. M. Man, D. Jones, D. Heldinger, C. H. Mastrangelo and D. T. Burke, *Science*, 1998, **282**, 484.
- 9 A. Garcia, L. K. Ista, D. N. Petsev, M. J. O'Brien, P. Bisong, A. A. Mammoli, S. R. J. Brueck and G. P. Lopez, *Lab Chip*, 2005, **5**, 1271.
- 10 S. S. Dukhin and B. V. Derjaguin, in *Equilibrium Double Layer and Electrokinetic Phenomena*, ed. E. Matijevic, Wiley-Interscience, New York, 1974.
- 11 R. J. Hunter, *Zeta Potential in Colloid Science*, Academic Press, New York, 1981.
- 12 P. Debye and E. Huckel, *Phys. Z.*, 1923, **24**, 185.
- 13 H. T. Davis, *J. Chem. Phys.*, 1986, **86**, 1474.
- 14 I. Bitsantis, J. J. Magda, M. Tirrell and H. T. Davis, *J. Chem. Phys.*, 1987, **87**, 1733.
- 15 I. Bitsantis, T. K. Vanderlick, M. Tirrell and H. T. Davis, *J. Chem. Phys.*, 1988, **89**, 3152.
- 16 K. P. Travis and K. E. Gubbins, *J. Chem. Phys.*, 2000, **112**, 1984.
- 17 K. P. Travis, B. D. Todd and D. J. Evans, *Phys. Rev. E: Stat. Phys., Plasmas, Fluids, Relat. Interdiscip. Top.*, 1997, **55**, 4288.
- 18 K. P. Travis, P. J. Daivis and D. J. Evans, *J. Chem. Phys.*, 1995, **103**, 1109.
- 19 J. B. Freund, *J. Chem. Phys.*, 2001, **116**, 2194.
- 20 R. Qiao and N. R. Aluru, *J. Chem. Phys.*, 2003, **118**, 4692.
- 21 A. P. Thompson, *J. Chem. Phys.*, 2003, **119**, 7503.
- 22 G. Karniadakis, A. Beskok and N. Aluru, *Microflows and Nanoflows*, ed. S. S. Antman, J. E. Marsden and L. Sirovich, Springer, New York, 2005.
- 23 Z. Yuan, A. L. Garcia, G. P. Lopez and D. N. Petsev, *Electrophoresis*, 2007, **28**, 595.
- 24 K. Ghowsi and R. J. Gale, *J. Electrochem. Soc.*, 1989, **136**, 867.
- 25 K. Ghowsi and R. J. Gale, *J. Chromatogr.*, 1991, **559**, 95.
- 26 K. Ghowsi and R. J. Gale, *Am. Lab.*, 1991, **23**, 17.
- 27 S. H. Zaidi, S. R. J. Brueck, F. M. Schellenberg, R. S. Mackay, K. Uekert and J. J. Persoff, *Interferometric Lithography Tool for 180-nm Structures*, SPIE, San Jose, USA, 1999, p. 2.
- 28 S. R. J. Brueck, in *There are No Fundamental Limits to Optical Lithography International Trends in Applied Optics*, ed. A. Guenther, SPIE Press, Bellingham, 2002.
- 29 M. J. O'Brien, P. Bisong, L. K. Ista, E. M. Rabinovich, A. L. Garcia, S. S. Sibbett, G. P. Lopez and S. R. J. Brueck, *J. Vac. Sci. Technol., B*, 2003, **21**, 2941.
- 30 J. Fu, P. Mao and J. Han, *Appl. Phys. Lett.*, 2005, **87**, 263902.
- 31 J. Han and H. G. Craighead, *Science*, 2000, **288**, 1026.
- 32 N. M. Ravindra and J. Zhao, *Smart Matter. Struct.*, 1992, **1**, 197.
- 33 S. R. Morrison, *Electrochemistry at Semiconductor and Oxidized Metal Electrodes*, Plenum Press, New York, 1980.
- 34 S. Levine, J. R. Marriot and K. Robinson, *J. Chem. Soc., Faraday Trans. 2*, 1975, **71**, 1.
- 35 L. D. Landau and E. M. Lifshitz, *Electrodynamics of continuous media*, Nauka, Moscow, 1982.
- 36 D. N. Petsev, G. P. Lopez, C. F. Ivory and S. S. Sibbett, *Lab Chip*, 2005, **5**, 587–597.
- 37 L. K. Ista, G. P. Lopez, C. F. Ivory, M. J. Ortiz, T. A. Schifani, C. D. Schwappach and S. S. Sibbett, *Lab Chip*, 2003, **3**, 266.
- 38 H. Cui, K. Horiuchi, P. Dutta and C. F. Ivory, *Anal. Chem.*, 2005, **77**, 7878.